

An Investigation on the Three Dimensional Vibration Characteristics of High-Speed Diesel Engine Crankshaft System with a Viscous Fluid Damper

Tomoaki KODAMA*, Katsuhiko WAKABAYASHI**,
Yasuhiro HONDA** and Shoichi IWAMOTO***

Abstract: The torsional vibration of diesel engines has become severer with the increase of exciting force by higher pressure. Therefore, the running crankshaft is highly stressed owing to the large torsional vibration. Then, torsional viscous fluid dampers of high performance have been employed in high mean effective pressure diesel engines as a measure for vibration reduction. As the dynamic characteristics of the dampers have such a great influence on the vibration of the engine crankshaft system that they cannot be ignored, the viscosity of the silicone oil and the peripheral and lateral gaps of the dampers are diversely varied in the experiment. As the equipment for the measurement of torsional vibration displacement, a phase-shaft type torsigraph equipment was adopted so as to make it easy to measure simultaneously angular displacements of the casing and the inertia ring. And the waveforms of axial and lateral vibrations were measured by non-contact micro-displacement vibrographs and laser displacement vibrographs. In the experiment, the 6 liters, 6 cylinders, in-line high-speed diesel engine whose vibration characteristics are known quite well was regarded as a vibration oscillator of the dampers. The dynamic characteristics of the high viscosity silicone oil damper and the optimum clearance between the casing and the inertia ring were investigated from a quantitative standpoint under full-load conditions, and the useful data in the design stage were gathered. As the result of the experimental study on the three-dimensional dynamic properties of torsional viscous fluid damper filled with silicone oil, the following conclusions are obtained;

- (1) The clearance value determined from BICERA's empirical formula is not always optimum on every viscosity of the filled silicone oil of the viscous fluid damper.
- (2) The optimum viscosity is different, due to the dimensions of the peripheral and lateral gaps between the outside of the inertia ring and the inside of the casing.
- (3) The effect of the amplitude reduction on the axial vibration of the crankshaft system with the typical torsional viscous fluid damper is small.
- (4) The lateral vibration are coupled with the torsional vibration of the crankshaft system.

Keywords: Diesel Engine, Viscous Fluid Damper, Torsional Vibration, Axial Vibration, Lateral Vibration, Peripheral Gap, Lateral Gap, Kinematic Viscosity

INTRODUCTION

Axial, torsional and two directions of lateral vibrations, which induce vibration stresses, occur simultaneously in the crankshaft system of a multi-cylinder engine [1]–[7]. The crankshaft of the multi-cylinder engine has a phase difference between the adjacent crank throw planes, so the four kinds of vibrations are all coupled in the crankshaft

system [1]–[7]. In recent years, the specific output has been increased and also the rigidity of the structure has been reduced in the high-speed automobile diesel engine. The torsional vibration of the crankshaft of the diesel engine with supercharger has especially become severer with increase of exciting force by high-pressure charging. Therefore the running crankshaft is highly stressed owing to the large torsional vibrations. At the same time the lateral vibration couple with the large torsional vibration occurs remarkably inside the operating engine speed range. Such being the case, it is necessary to add vectorially the bending vibration stress to the torsional vibration stress in order to calculate the resultant stress[1]–[7]. It has thus become much more important to estimate all the vibration stresses accurately, including some kinds of coupled vibration in the design stage. On the other hand, typical tor-

* Technical Staff, Department of Mechanical Engineering and Applied Information Technology, Faculty of Engineering

** Professor, Department of Mechanical Engineering and Applied Information Technology, Faculty of Engineering, Dr. of Engineering

*** Advanced Research Institute for Science and Engineering, Waseda University, Dr. of Engineering

sional viscous fluid dampers consist of an annular seismic-mass enclosed in a casing. The peripheral and lateral gaps between these two members are filled with a viscous fluid, e.g. dimethyl silicone fluid, and the thin layer is formed. As the silicone fluid is non-Newtonian fluid, the effective viscosity in the actuation is different from that in the operating condition and the complicated characteristics are shown. The damping not only is improved with the increase of the viscosity of filled silicone fluid, but also the complex damping combined with the elasticity increases. In addition, velocity gradient arises in the silicone fluid layer between the damper casing and the inertia ring, when torsional vibration is generated, and the vibration energy is dissipated as the heat energy by the shear resistance [8]–[27]. Therefore, the clearance dimension between the inside of the casing and the outside of the inertia ring becomes an important subject in the viscous damper design [8]–[27]. In addition, these factors have a great effect on the torsional, axial and lateral vibrations characteristics of the crankshaft system. Then, the experiments of torsional vibration characteristics were carried out under these conditions of the changes of the viscosity and the gap dimension of the viscous damper in an automotive diesel engine. The torsional vibration angular displacement waveforms were simultaneously measured in two points of the damper casing and the inertia ring. It is the purpose to calculate directly the dynamic values from the measured waveforms and to make their characteristics clear.

MECHANISM OF COUPLED TORSIONAL-LATERAL VIBRATION ON A RECIPROCATING ENGINE CRANKSHAFT SYSTEM

This chapter refers to the mechanism of the lateral vibration coupled with the torsional vibration. Fig. 1 shows a one throw skeleton model of a crankshaft. *O*-point is the origin of coordinates and the *x*, *y* and *z* principal axes are shown in Fig. 1. The coordinate system in this paper is presented in the right-hand rectangular coordinate system. It is assumed that the model of the crank is simply supported in the *y*, *z* direction and the equilibrium of forces is considered. When a lateral force in the *y* direction *F_y* is applied, a lateral displacement in the *y* direction

v is produced. The a lateral force *F_y* causes a bending moment in the *z* direction *M_z* on the *O*-point and an angular displacement in the *z* direction *φ* is produced. As the lateral force *F_y* brings simultaneously about a torsional moment in the *x* axis, it is necessarily supported by a moment in the *x* direction *M_x*. The moment caused by the inertia force on the basis of the acceleration of the flywheel, the pulley and the remaining mass parts balances with the torsional moment on the *x* axis. When the lateral vibromotive force in the *y* direction *F_y* is applied, the lateral vibration in the *z* axis and the torsional vibration in the *x* axis are produced at the same time. These phenomena prove that the coupled torsional-lateral vibration occurs in the multi-cylinder, reciprocating engine shaft system. When a lateral force in the *z* direction is applied, a different coupled vibration is produced. The coupled vibrations of other throws are caused in the same way as was stated previously. In addition to that, the crankshaft of the multi-cylinder engine has a phase difference between the adjacent crank throw planes, so four kinds of vibrations are all coupled in the crankshaft system.

SPECIFICATIONS OF EXPERIMENTAL ENGINE

The test engine used for the measurement of vibration displacements is the 6 cylinders, in-line, automotive high-speed diesel engine. The main specifications of the test engine are shown in Table 1.

GEOMETRICAL DIMENSION OF VISCOUS FLUID DAMPER

GEOMETRICAL DIMENSION OF STANDARD DESIGN VISCOUS-FLUID DAMPER

The engine crankshaft system with a viscous damper is replaced with the equivalent vibration system. The effective mass moment of inertia *I_e*(=0.011 kgm²)and the natural angular velocity *ω_e* of the engine crankshaft system can be obtained by Holzer’s method. Then, the inertia moment of damper inertia ring *I_d*(=0.330 × 10⁻² kgm²) can easily be calculated on the assumption that the damper inertia ratio *R*(=*I_d*/*I_e*) is equal to 0.3 [18],[23]–[27]. The clearance *δ* of the standard viscous damper is mostly de-

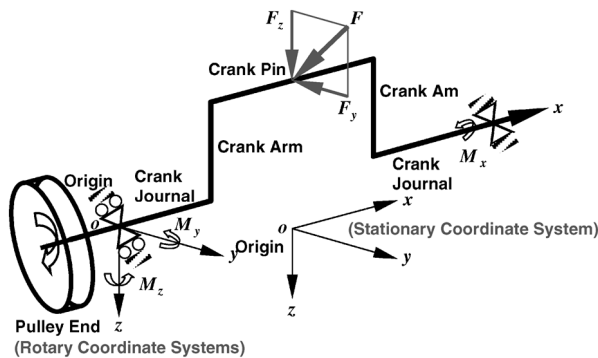


Fig. 1 Skeleton Vibration Model of Crank Throw and Pulley End

Table 1 Main Specifications of the Test Engine

| Particulars | Contents | |
|---------------------------|----------------------------------|---------------|
| Designed for | High-Speed Diesel Engine | |
| Type for | 4-Stroke Cycle, Direct Injection | |
| Number of Cylinders | 6-Cylinders | |
| Arrangement | In-Line | |
| Bore and Stroke | m | 0.105 - 0.125 |
| Total Piston Displacement | m ³ | 0.006469 |
| Compression Ratio | 17.0 | |
| Maximum Brake Output | kW/r/min | 230 / 3200 |
| Maximum Brake Torque | Nm/r/min | 451 / 1800 |
| Firing Order | 1 - 5 - 3 - 6 - 2 - 4 | |

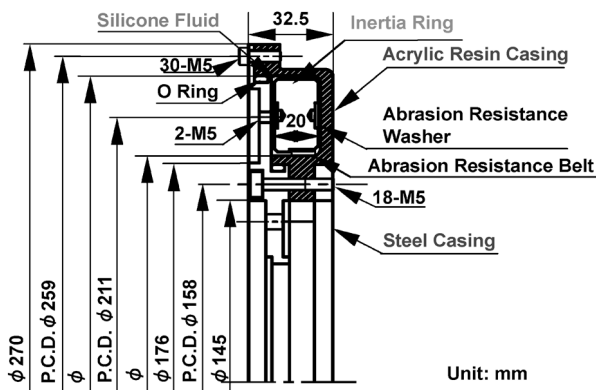


Fig. 2 Shape and Dimensions of Test Viscous Fluid Damper

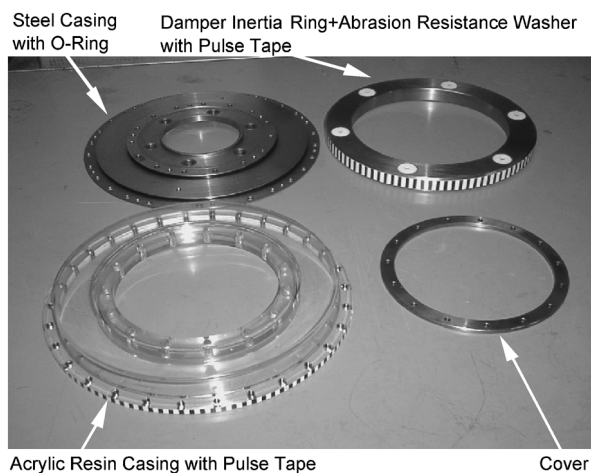


Photo 1 Component Parts of Test Viscous Fluid Damper

terminated from the BICERA's empirical formula shown in the following [28].

$$\delta = 0.010 + 0.010 \times \sqrt{\left(\frac{D_0}{10}\right)} \text{ [inch]} \quad (1)$$

Where, D_0 : outer diameter of damper inertia ring. The clearance is determined to be approximately 0.0197 inch = 0.50 mm by substituting $D_0 (= 241.00 \text{ mm}) = 9.49 \text{ inch}$ into equation (1). Then, the inside diameter of the casing becomes 242.00 mm. The dimension and the shape of the standard viscous damper shown in Fig. 2 were decided by considering those of the dampers widely adopted in the high speed diesel engines until the present. Photo 1 shows the component parts of the test viscous-fluid damper.

GEOMETRIES OF VARIOUS VISCOUS FLUID DAMPERS

As shown in Tables 2(a), 2(b) and 3, the dimensions of the inertia rings and the viscosities of the silicone fluids, respectively, were diversely varied in this experiment, in order to investigate the dynamic characteristics of the viscous dampers. The number of the inertia ring of the standard viscous damper is No. 02-S* in Tables 2(a), and (b). The clearance of the standard damper were determined from the BICERA's empirical formula [28]. The peripheral and lateral gaps between the inertia ring and the casing

Table 2(a) Dimensions of Damper Inertia Rings (Lateral Gap: Change, Peripheral Gap: Constant)

| Number of Inertia Ring | Moment of Inertia $\times 10^{-2} \text{ kgm}^2$ | Thickness $\times 10^{-2} \text{ m}$ | Outside Radius $\times 10^{-1} \text{ m}$ | Inside Radius $\times 10^{-2} \text{ m}$ |
|------------------------|--|--------------------------------------|---|--|
| No. 01-L | 3.256 | 1.940 | 1.205 | 9.040 |
| No. 02-S* | 3.200 | 1.900 | 1.205 | 9.040 |
| No. 03-L | 3.029 | 1.800 | 1.205 | 9.040 |
| No. 04-L | 2.882 | 1.700 | 1.205 | 9.040 |
| No. 05-L | 2.723 | 1.600 | 1.205 | 9.040 |
| No. 06-L | 2.564 | 1.500 | 1.205 | 9.040 |

Table 2(b) Dimensions of Damper Inertia Rings (Peripheral Gap: Change, Lateral Gap: Constant)

| Number of Inertia Ring | Moment of Inertia $\times 10^{-2} \text{ kgm}^2$ | Thickness $\times 10^{-2} \text{ m}$ | Outside Radius $\times 10^{-1} \text{ m}$ | Inside Radius $\times 10^{-2} \text{ m}$ |
|------------------------|--|--------------------------------------|---|--|
| No. 01-P | 3.229 | 1.900 | 1.207 | 9.040 |
| No. 02-S* | 3.200 | 1.900 | 1.205 | 9.040 |
| No. 03-P | 3.115 | 1.900 | 1.200 | 9.040 |
| No. 04-P | 3.031 | 1.900 | 1.195 | 9.040 |
| No. 05-P | 2.960 | 1.900 | 1.190 | 9.040 |
| No. 06-P | 2.890 | 1.900 | 1.185 | 9.040 |

Table 3 Viscosity of Silicone Fluid

| Number of Silicone Fluid | Kinematic Viscosity m^2/s |
|--------------------------|---|
| No. 0 1 | 5.0×10^{-2} |
| No. 0 2 | 1.0×10^{-1} |
| No. 0 3 | 3.0×10^{-1} |

were changed on the basis of those of the standard damper.

SIMULTANEOUS MEASUREMENT OF TORSIONAL ANGULAR DISPLACEMENT AND AXIAL, LATERAL DISPLACEMENT WAVEFORM

The test engine was equipped with the torsional viscous fluid damper. An eddy-current dynamometer was connected to the crankshaft of the engine via an intermediate shaft and a universal joint. The torsional vibration waveforms were simultaneously measured at the outsides of the inertia ring and the casing. Transparent acrylic resin suitable for penetrating light was adopted as the material of the casing part. The tapes, in which white and black parts were arranged alternately for generating signal pulses, were stuck in the outsides of the casing and the inertia ring. The floodlight from the light emission division of the photo sensor and the reflected light were detected by the light-receiver. The electric frequency signals proportional to engine speed were obtained from the photo pickup. The measured signals were transmitted to the phase-shift torsionograph equipment via the adapter which calculated the average of angular velocity (the center frequency). The torsional vibration waveforms could be obtained from the torsional angles, which were calculated using the relation-

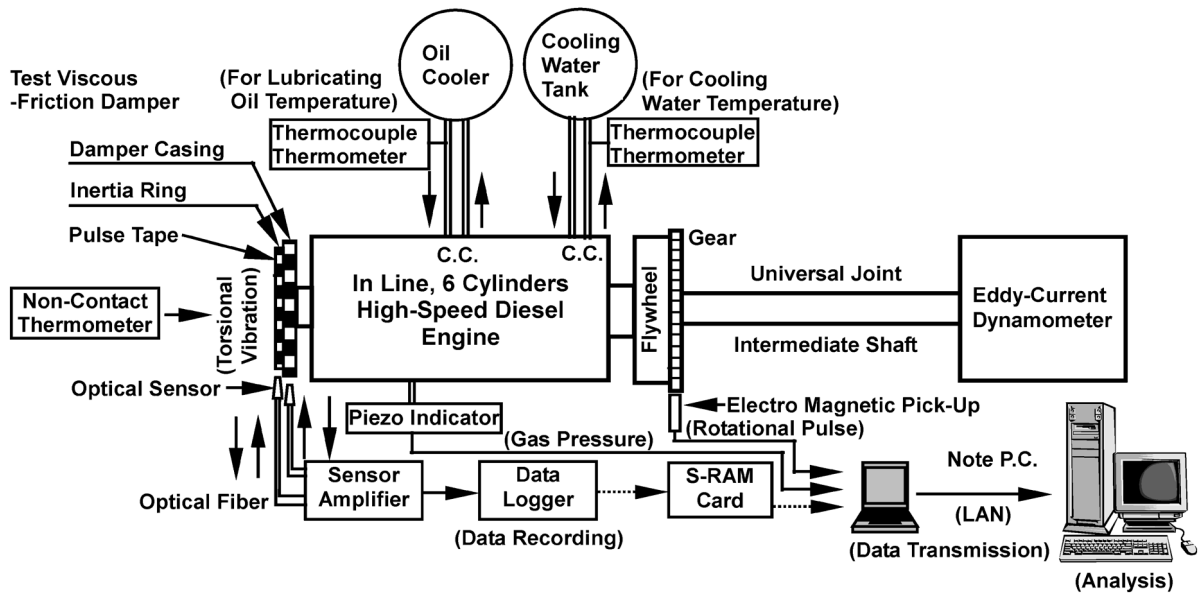


Fig. 3(a) Schematic Diagram of Simultaneously Measuring of Torsional Vibration Waveforms at Two Points

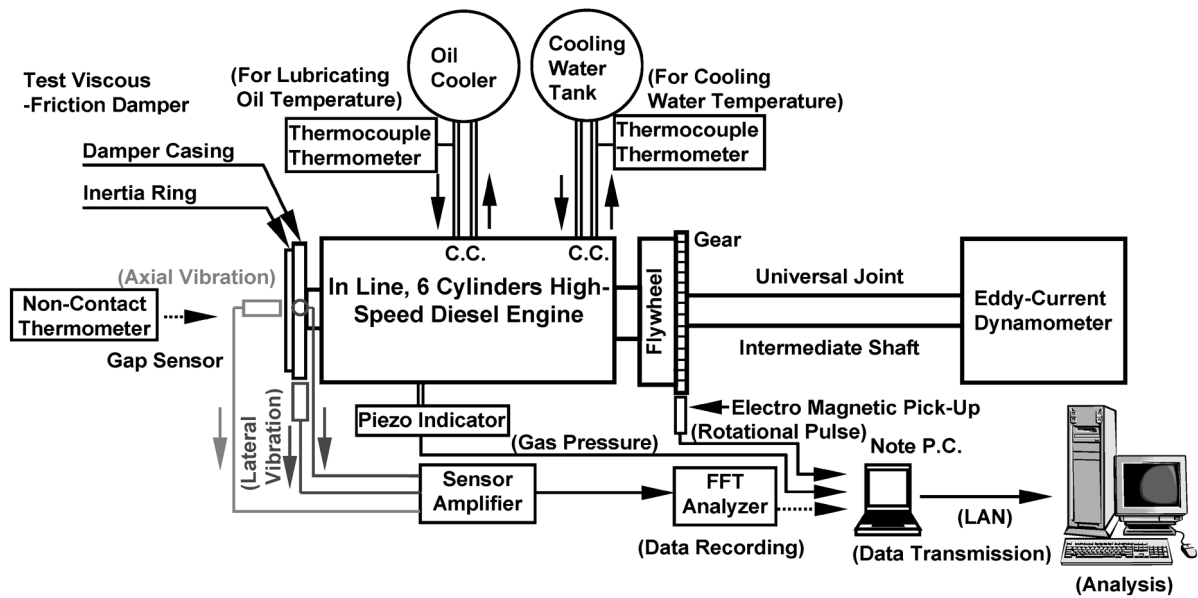


Fig. 3(b) Schematic Diagram of Measuring System of Axial and Lateral Vibrations Waveforms

ship between the measured and center frequencies. The signals were recorded by the data logger via the amplifier. The measured torsional waveforms of the damper inertia ring and the casing were harmonically analyzed using the F.F.T. analyzer. The schematic drawings of the experimental system are shown in Fig. 3(a) and (b). As this method can simultaneously measure the waveforms of the damper inertia ring and the casing, it is an advantage to be able to calculate directly the dynamic characteristics of silicone oil. The waveforms of axial and lateral vibrations were measured by non-contact microdisplacement vibrograph (hereafter called “gap sensor”) and laser displacement vibrograph. Voltage signal proportional to the measured values of the axial and lateral vibration waveform

was taken out by the sensors which were installed in the front surface and on the circumference, respectively. The electric signals were amplified by the amplifier and recorded by the data logger. The measured waveforms of the damper inertia ring and casing were harmonically analyzed using the FFT analyzer. Besides, the lateral vibration displacement is measured by gap sensors and laser displacement vibrographs located on the stationary coordinate system. But the real lateral vibration occurs on the rotary coordinate system of the rotating crankshaft. Therefore, it is necessary to transform the actual experimental data into the value in the rotary coordinate system. The torsional, axial and lateral vibrations waveforms were measured under full load from 1000 to 3000 r/min.

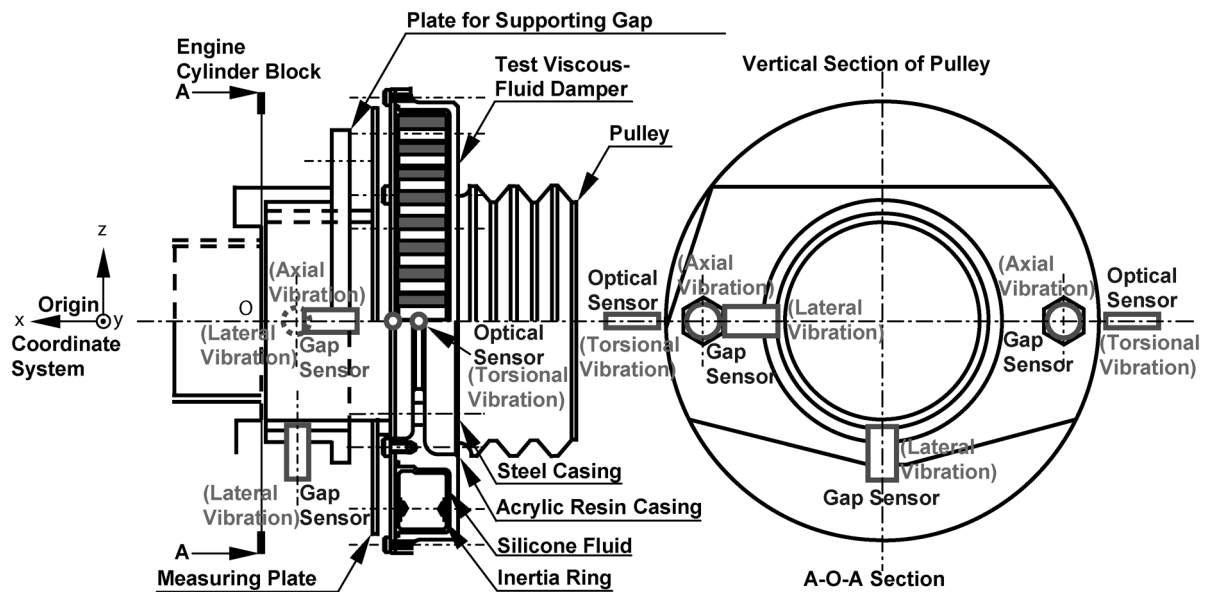


Fig. 4 Devices for Measuring Torsional, Axial and Lateral Vibration Displacements and their Clamping Location

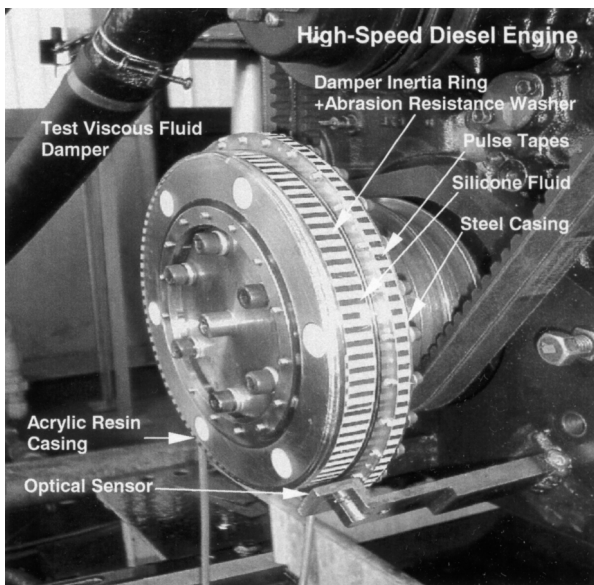


Photo 2 Simultaneously Measurement of Torsional Vibration Waveforms at Two Points

The temperatures of the cooling water and the lubricating oil of the engine kept constant, and also the surface temperature of the viscous fluid damper was retained at the approximately fixed 333 K in the experiments. The experiments in this study are made to obtain the displacement waveforms of torsional, axial and two directions of lateral vibrations at the pulley end of the test engine. Fig. 4 illustrates the setting locations of the devices for measuring torsional, axial and lateral displacement. Photo 2 shows the test viscous-friction damper attached diesel engine. The tapes were stuck in the outside of the damper casing and the inertia ring

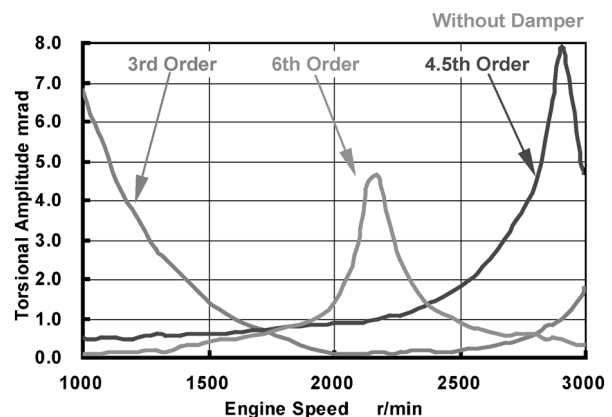


Fig. 5 Measured Amplitude Curves of Torsional Angular Displacements at Pulley End (Without Viscous Fluid Damper)

MEASUREMENT RESULTS OF AMPLITUDE OF TORSIONAL ANGULAR, AXIAL AND LATERAL DISPLACEMENTS

IN CASE OF NON-EQUIPMENT OF A VISCOUS FLUID DAMPER

Fig. 5 illustrates the measured amplitude curves of the torsional vibration displacements at the pulley end of the crankshaft system without the viscous fluid damper. The measured vibration waveforms were harmonically analysed and the values of the each order components were adopted for getting the torsional amplitude curves. The 4.5th and 6th order resonance points of the 2nd-node torsional vibrations appear mainly at 2900 and 2170 r/min, respectively, within running engine speed. The values of their resonance amplitudes are 7.8 and 4.6 mrad,

respectively. In addition, the skirt of the 3rd order resonance curves has appeared in the region of low engine speed. These are the major critical orders of the 6 cylinders engine. Fig. 6 shows the amplitude curves of the axial vibration displacements at the pulley end of the crankshaft system without the viscous fluid damper. The 5th order vibration has a maximum resonance amplitude of 5.2×10^{-1} mm and its resonance point appear at 2320 r/min. Fig. 7 illustrates the amplitude curves of the lateral vibrations, in the z direction, at the pulley end of the crankshaft system without the viscous fluid damper. As the lateral vibration displacements at the pulley end were measured in a fixed coordinate system located on the engine block, coordinate transformation was performed from the stationary to the rotary coordinate system. The 6th order vibration has a maximum resonance amplitude of 7.9×10^{-1} mm and its resonance point at 2490 r/min.

IN CASE OF EQUIPMENT OF VISCOUS FLUID DAMPER

Fig. 8(a), (b) and (c) show the measured amplitude curves of the torsional vibration displacements in the damper casing. The 4.5th and 6th order resonance points of the torsional vibrations appear within running engine speed, but their resonance amplitudes are greatly reduced

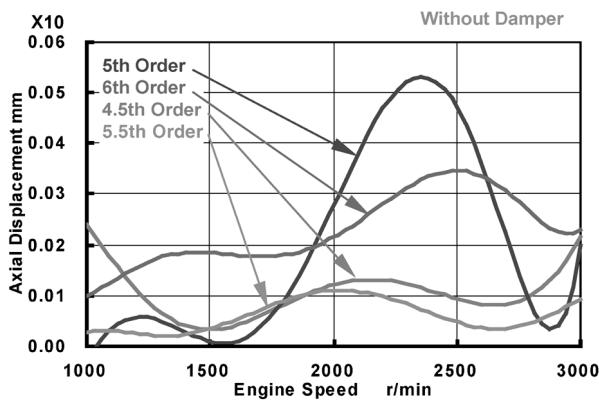


Fig. 6 Measured Amplitude Curves of Axial Displacement at Pulley End (Without Viscous Fluid Damper)

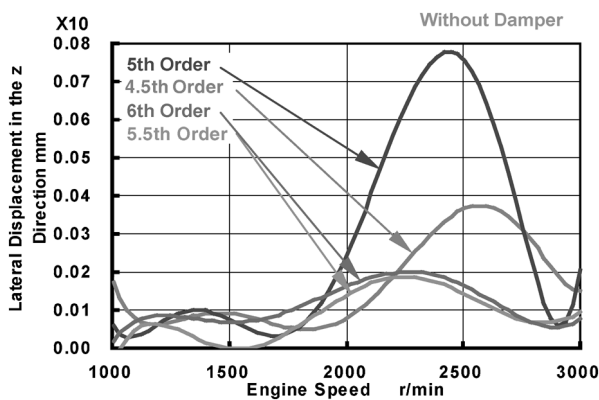


Fig. 7 Measured Amplitude Curves of Lateral displacement in the z Direction at pulley End (Without Viscous Fluid Damper)

by employing the viscous fluid damper in comparison with those without damper. In addition, Fig. 9(a), (b) and (c) show the amplitude curves of the axial vibration displacements at the pulley end of the crankshaft system with the

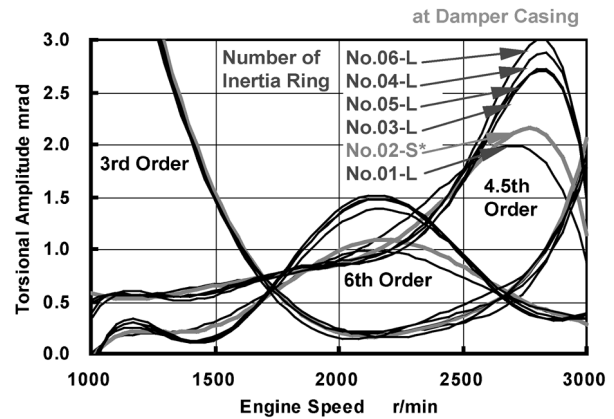


Fig. 8(a) Measured Amplitude Curves of Torsional Angular Displacements of Damper Casing on Condition of Lateral Gap Changes (Kinematic Viscosity: 0.05 m²/s)

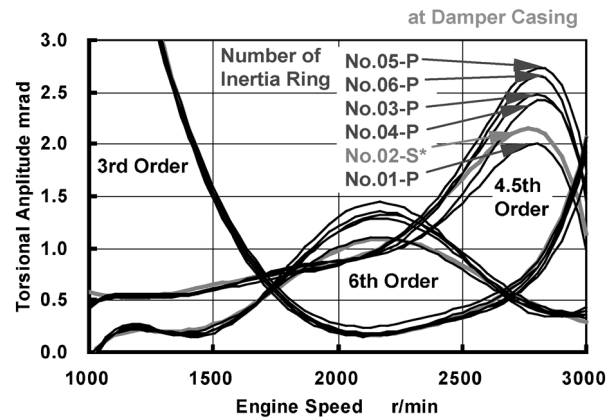


Fig. 8(b) Measured Amplitude Curves of Torsional Angular Displacements of Damper Casing on Condition of Peripheral Gap Changes (Kinematic Viscosity: 0.05 m²/s)

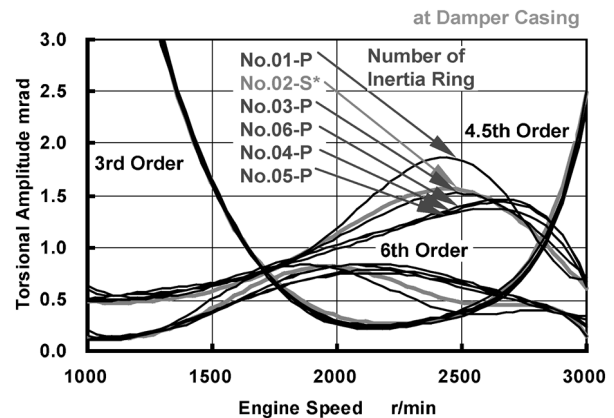


Fig. 8(c) Measured Amplitude Curves of Torsional Angular Displacements of Damper Casing on Condition of Peripheral Gap Changes (Kinematic Viscosity: 0.30 m²/s)

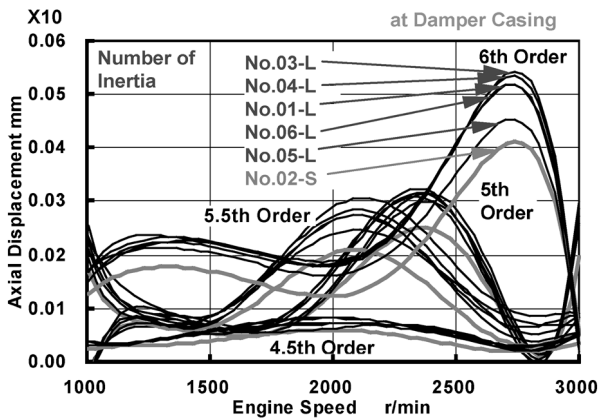


Fig. 9(a) Measured Amplitude Curves of Axial Displacements of Damper Casing on Condition of Lateral Gap Changes (Kinematic Viscosity: 0.05 m²/s)

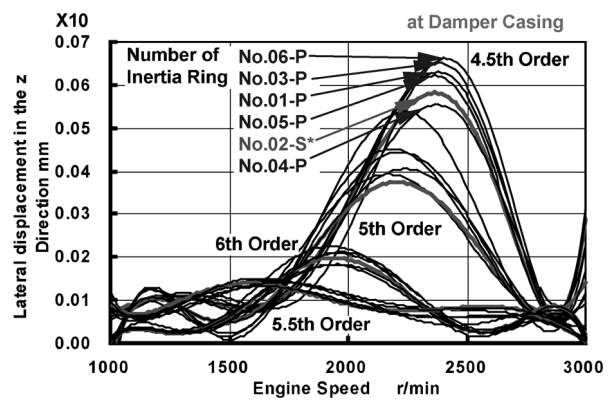


Fig. 10(a) Measured Amplitude Curves of Lateral Displacements in the z Direction of Damper Casing on Condition of Peripheral Gap Changes (Kinematic Viscosity: 0.05 m²/s)

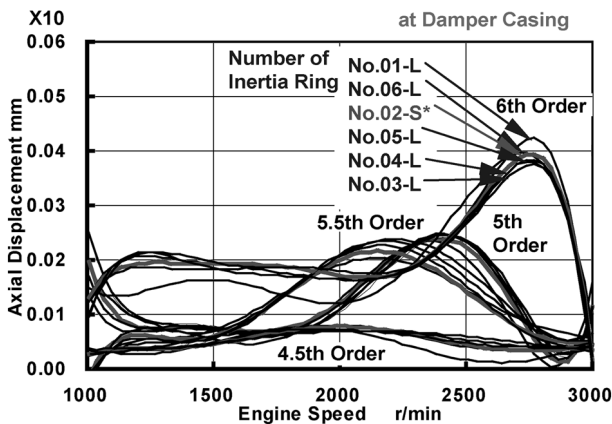


Fig. 9(b) Measured Amplitude Curves of Axial Displacements of Damper Casing on Condition of Lateral Gap Changes (Kinematic Viscosity: 0.10 m²/s)

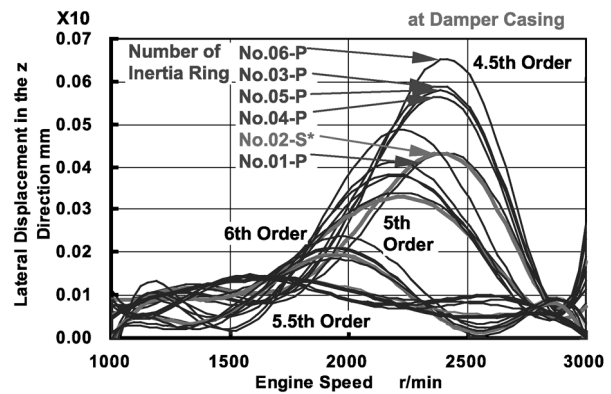


Fig. 10(b) Measured Amplitude Curves of Lateral Displacements in the z Direction of Damper Casing on Condition of Peripheral Gap Changes (Kinematic Viscosity: 0.10 m²/s)

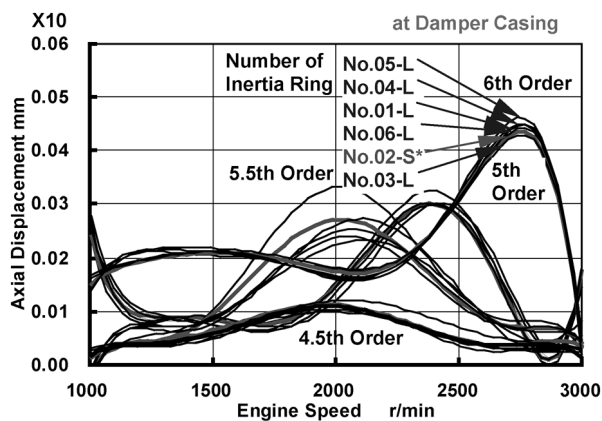


Fig. 9(c) Measured Amplitude Curves of Axial Displacements of Damper Casing on Condition of Lateral Gap Changes (Kinematic Viscosity: 0.30 m²/s)

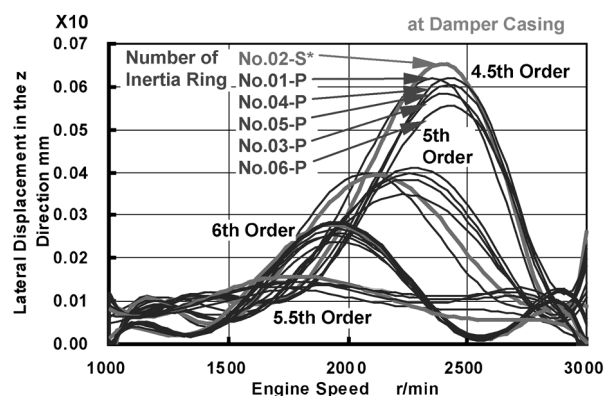


Fig. 10(c) Measured Amplitude Curves of Lateral Displacements in the z Direction of Damper Casing on Condition of Peripheral Gap Changes (Kinematic Viscosity: 0.30 m²/s)

viscous fluid damper. It is shown that the 5th order resonance amplitude is reduced by employing the damper. However, the 5.5th and 6th order resonance amplitudes are increased. The decreasing effect of the 4.5th order resonance amplitude has not appeared. The values of the resonance amplitudes are not always reduced on each ord-

er axial vibration by changing from the low to high viscosity of the filling silicone oil. The values of the axial vibration displacements have a tendency to be reduced by increasing the lateral gap. Fig. 10(a), (b) and (c) shows the measured amplitude curves of the lateral vibration in the z direction at the pulley end of the crankshaft system with

the viscous fluid damper. The 6th order resonance amplitude is greatly reduced by fitting the viscous fluid damper, but the 5.5th order resonance amplitude becomes larger. And, the 6.5th and 7th order resonance amplitudes is not reduced. The factors of the viscosity, the peripheral gap and the lateral gap don't have remarkably influence on the reduction of the lateral vibration.

INVESTIGATION OF MEASUREMENT RESULTS OF TORSIONAL ANGULAR, AXIAL AND LATERAL DISPLACEMENTS

INVESTIGATION OF EXPERIMENTAL RESULTS OF TORSIONAL ANGULAR DISPLACEMENTS

As some experimental results of torsional angular displacements, Fig. 8(a), (b) and (c) have been already shown. As the summary of the all results, the value of the resonance amplitude is reduced on each major critical order vibration, when the viscosity of silicone oil is changed from the low to high viscosity. And, it is shown that the engine speed of each order resonance point also changes. These phenomena originate from the change of the dynamic characteristic values by varying the viscosity of the filled silicone oil. The peripheral gap between the damper casing and inertia ring have much more effect on the reduction of torsional vibration amplitude than the lateral gap. Next, Fig. 11(a) and (b) illustrates the relationship between the resonant torsional amplitude and the clearance dimension on conditions of the changes of the only lateral gap. As shown in Table 3, the viscosity of the silicone oil is diversely varied in this experiment. The clearance dimension of less than 0.5 mm in the range of the low viscosity of the silicone oil is more effective on the reduction of the resonant torsional amplitude than the clearance dimension of 0.5 mm given by BICERA's empirical formula [28]. But the resonant torsional amplitude in the clearance dimension of more than 0.5 mm become larger in the range of the high viscosity of the filling silicone oil than that in the clearance dimension of 0.5 mm. And, the optimum clearance dimension of the damper with the viscosity of 0.1 m²/s is nearly 0.5 mm.

INVESTIGATION OF EXPERIMENTAL RESULTS OF AXIAL VIBRATION DISPLACEMENTS

The natural frequencies of the torsional vibrations of the 4.5th and 6th orders are clearly different from those of the axial vibrations of the corresponding orders. Then, these axial vibrations don't couple with the torsional vibrations. In addition, it is shown that the axial vibration coupled with the torsional vibration does not exist. This is based on the structure of the test engine crankshaft. The effect of the viscous fluid damper on the reduction of the axial vibration has already mentioned on the previous chapter. It is difficult to reduce all orders amplitudes of the axial vibration displacements by employing the damper. However, if the inertia ring enclosed in the damper casing can sufficiently move to the axial direction, it is supposed to be possible to reduce the amplitude of the axial vibration displacement.

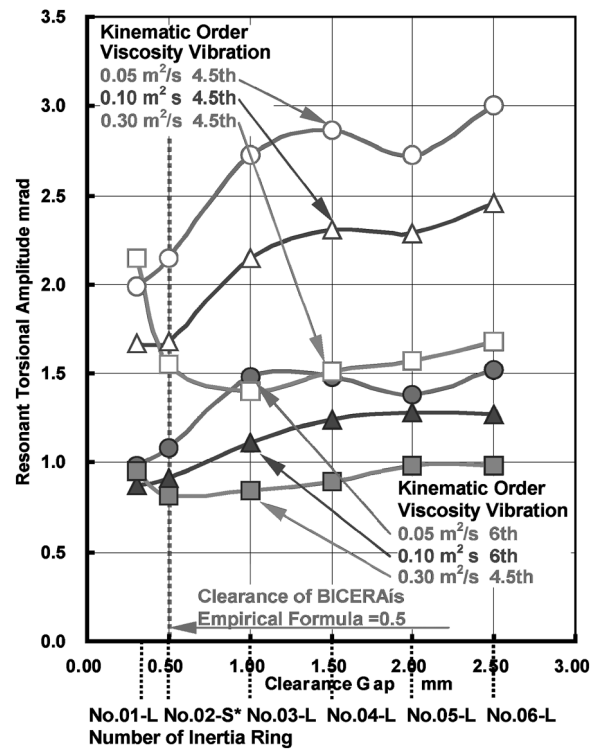


Fig. 11(a) Relationship between Resonant Torsional Amplitude and Clearance Gap (Lateral Gap: Change, 4.5th and 6th Order Vibrations)

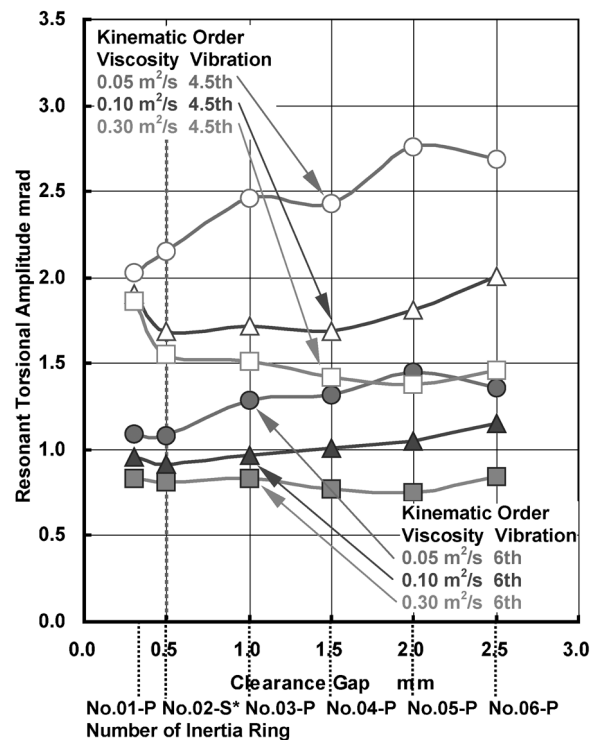


Fig. 11(b) Relationship between Resonant Torsional Amplitude and Clearance Gap (Peripheral Gap: Change, 4.5th and 6th Order Vibrations)

INVESTIGATION OF EXPERIMENTAL RESULTS OF LATERAL VIBRATION DISPLACEMENTS

As the effect of the viscous fluid damper on the reduction of the lateral vibration has already described in the previous chapter, it is difficult to reduce remarkably the lateral vibration. The factors of the viscosity, the peripheral gap and the lateral gap don't have remarkable influence on the reduction of the lateral vibration. This results originates in the structure of the viscous damper, because the inertia ring enclosed in the damper casing cannot sufficiently move to the transverse direction. Then, it is necessary to change the structure of the damper.

INVESTIGATION OF LATERAL VIBRATION COUPLED WITH TORSIONAL VIBRATION

In order to investigate the characteristics of the lateral vibration coupled with the torsional vibration, we must pay our attention to the 6th order component of the lateral vibrations in the rotary coordinate system, because the 6th order components of the torsional vibrations which are the major critical order. When the experimental results of the torsional vibrations without and with a damper are compared with those of the lateral vibrations without and with a damper, the engine speed of the torsional resonance points agree with those of the corresponding lateral resonance points. Besides, both the 6th resonance amplitudes of the torsional vibrations and the lateral vibrations are greatly reduced by employing the viscous fluid damper. Then, the 6th lateral vibration is coupled with the 6th torsional vibration.

CONCLUSIONS

The experiments, in which the clearance dimensions of the peripheral, lateral gap filled with viscous fluid and also the kinematic viscosity of its silicone fluid were diversely varied, were been carried out and the torsional angular, axial and lateral vibration displacements at the damper inertia ring and the casing were measured simultaneously. As the results of the experiments on the dynamic properties of the viscous fluid dampers, the following conclusions are obtained;

- [1] The clearance value determined from BICERA's empirical formula is not always optimum on every viscosity of the filled silicone oil of the viscous fluid damper.
- [2] The optimum viscosity is different by the dimensions of the peripheral and lateral gaps between the outside of the inertia ring and the inside of the casing.
- [3] The effect of the amplitude reduction on the axial vibration of the crankshaft system with the typical torsional viscous fluid damper is small.
- [4] The values of the resonance amplitudes of the axial vibration are not always reduced by changing from the low to high viscosity of the silicone oil.
- [5] The lateral vibration of the 6th order are coupled with the torsional vibration of this crankshaft system.

REFERENCES

- [1] Katsuhiko Wakabayashi, Yasuhiro Honda, Tomoaki Kodama Shoichi Iwamoto, "The Characteristics of Bending Vibration Stress Coupled with Torsional Vibration of Automotive Diesel Engine Shaftings", *1995 SAE International Congress and Exposition, SAE Paper No. 950543* (1995) P. 23-39.
- [2] Katsuhiko Wakabayashi, Kunio Shimoyamada, Tomoaki Kodama, Shoichi Iwamoto, "A Study on the Characteristics of Bending Vibration Coupled with Torsional Vibration in the Crankshafting of a V-Type, 8 Cylinder Diesel Engine", *Transactions of Kokushikan University, Faculty of Engineering*, (in Japanese), No. 18 (1985) P. 35-39.
- [3] Katsuhiko Wakabayashi, Shoichi Iwamoto, Tomoaki Kodama, Yasuhiro Honda, "An Investigation of Three-Dimensional Vibrations of Diesel Engine Shaftings Using the Transfer Matrix Method", *Journal of the Marine Engineering Society in Japan*, (in Japanese), Vol. 31, No. 9 (1996) P. 670-678.
- [4] Katsuhiko Wakabayashi, Yasuhiro Honda, Tomoaki Kodama, Shoichi Iwamoto, "Three Dimensional Analysis of Forced Vibrations of Diesel Engine Shaftings by the Transfer Matrix Method", *Proceedings of International Symposium on Marine Engineering Yokohama '95*, Vol. II (1995) P. 35-42.
- [5] Katsuhiko Wakabayashi, "A 3-Dimensional Analysis of Forced Vibrations of Reciprocating Engine Shaftings", *Internal Combustion Engine*, (in Japanese), Vol. 29, No. 365 (1990) P. 44-50.
- [6] Takeo Naganuma, Hideo Okamura, Kiyoshi Sogabe, "Experiments and Analyses of the Three-Dimensional Vibrations of the Crankshaft and Torsional Damper in a Four-Cylinder In-Line High Speed Engine", *SAE Noise and Vibration Conference, SAE Paper No. 971996* (1996) P. 1009-1020.
- [7] Abdulla S. Rangwala, "*Reciprocating Machinery Dynamics Design and Analysis*", Marcel Dekker, Inc., (2001) P. 400-466, New York.
- [8] Shoichi Iwamoto, "Study on the Effective Viscosity of Working Oil in Viscous Torsional Vibration Damper of Diesel Engine, Second Report: Complex Viscosity of Working Oil in Damper of High Speed Engine", *Journal of the Marine Engineering Society in Japan*, (in Japanese), Vol. 18, No. 10 (1983) P. 795-800.
- [9] Shoichi Iwamoto, Tohru Yonezawa, Yasunori Mukawa, "Study on the Effective Viscosity of Working Oil in Viscous Torsional Vibration Damper of Diesel Engine, Third Report: Complex Viscosity of Working Oil in Damper of Low Speed Engine", *Journal of the Marine Engineering Society in Japan*, (in Japanese), Vol. 18, No. 12 (1983) P. 975-981.
- [10] Masao Sugimoto, Hideo Ohashi, Toshihiro Takenaka, "Dynamic Damper with Damping for Torsional Vibration", *Journal of the Marine Engineering Society in Japan*, (in Japanese), Vol. 18, No. 10 (1983) P. 993-998.
- [11] Katsuhiko Wakabayashi, Shoichi Iwamoto, Kunio Shimoyamada, "Analysis of Vibrations of Reciprocating Engine Shaftings by the Transfer Matrix Method, The Fourth Report: Torsional Vibration Stress of a Crankshaft with a Viscous Fluid Damper", *Journal of the Marine Engineering Society in Japan*, (in Japanese), Vol. 19, No. 1

(1984) P. 24–33.

[12] Toshihiko Asami, Kyosuke Iribem Kazunari Momose, Yoshinobu Hosokawa, “Effect of Compressibility of Oil on an Oil Damper” *Transactions of the Japan Society of Mechanical Engineers*, (in Japanese), No. 91–1344, Vol. 58, No. 549, C (1992) P. 1592–1600.

[13] Yuichi Sato, Naoki Moriguchi, “Suppression of Torsional Vibrations by a Partitioned Hollow Rotor Containing Liquid”, *Transactions of the Japan Society of Mechanical Engineers*, (in Japanese), No. 92–0858, Vol. 59, No. 557, C (1993) P. 17–23.

[14] Yuichi Sato, Kengo Koshimizu, “Suppression of Torsional Vibrations by a Sectored Hollow Cylinder Containing”, *Transactions of the Japan Society of Mechanical Engineers*, (in Japanese), No. 93–0939, Vol. 59, No. 569, C (1994) P. 44–49.

[15] Ikuo Shimoda, “Study of High Viscous Damper: Modeling of Viscoelasticity and Proposition of Design Method”, *Transactions of the Japan Society of Mechanical Engineers*, (in Japanese), No. 93-1098, Vol. 60, No. 570, C (1994) P. 44–49.

[16] Takahiro Yamauchi, Yukimi Yamazaki, “Computation and Experiment Analysis for Torsional Vibration of Crankshaft System with Viscous Torsional Damper”, *Isuzu Technical Review*, (in Japanese), No. 100 (1998) P. 112–119.

[17] Shoichi Iwamoto, Katsuhiko Wakabayashi, Tomoaki Kodama, “A Study for the Characteristics of Torsional Vibration Damping in High-Speed Diesel Engine, The Third Report: Engine Damping in an Engine System with a Viscous Torsional Vibration Damper”, *The Science and Engineering Reports of Saitama University*, (in Japanese), No. 16, C (1983) P. 15–19.

[18] Katsuhiko Wakabayashi, Kunio Shimoyamada, Tomoaki Kodama, Shoichi Iwamoto, “A Study on the Torsional Vibration Characteristics of Crankshaftings with a Viscous Fluid Damper, The First Report: Complex Damping Coefficient of Dampers”, *Transactions of Kokushikan University, Faculty of Engineering*, (in Japanese), No. 17 (1984) P. 54–62.

[19] Katsuhiko Wakabayashi, Yasuhiro Honda, Tomoaki Kodama, Shoichi Iwamoto, “The Dynamic Characteristics of Torsional Viscous-Friction Dampers on Reciprocating Engine Shaftings”, *SAE 1992 Transactions, Journal of Engines*, Section 3 Vol. 101, SAE Paper No. 921726 (1993) P. 1734–1754.

[20] Katsuhiko Wakabayashi, Yasuhiro Honda, Tomoaki Kodama, Shoichi Iwamoto, “The Effect of Typical Torsional Viscous-Friction Damper on the Reduction of Vibrations in the Three Dimensional Space of Diesel Engine Shaftings”, *SAE 1993 Transactions, Journal of Engines*, Section 3, Vol. 102, SAE Paper No. 932009.

[21] Katsuhiko Wakabayashi, Kunio Shimoyamada, Tomoaki Kodama, Yasuhiro Honda, Shoichi Iwamoto, “A Study of Torsional Vibration Characteristics of Diesel Engine Shaftings with a Viscous Fluid Damper”, *Proceedings of Japan Society Automotive Engineers*, (in Japanese), No. 912252 (1991) P. 373–376.

[22] Katsuhiko Wakabayashi, Yasuhiro Honda, Tomoaki Kodama, Hirishi Okamura, “Study on Optimum Torsional Viscous-Friction Damper”, *Proceedings of the Japan Society of Mechanical Engineers, Dynamics and Design Con-*

ference ’98, (in Japanese), No. 98–8 I, Vol. A (1998) P. 92–95.

[23] Katsuhiko Wakabayashi, Takayuki Haraguchi, Tomoaki Kodama, Shoichi Iwamoto, “An Investigation into the Dynamic Characteristics of Torsional Viscous-Friction Dampers by Simultaneous Measurement at Two Points”, *Proceedings of the 6th International Symposium on Marine Engineering Tokyo*, No. 2000–TS–089, (2000) P. 569–576.

[24] Tomoaki Kodama, Katsuhiko Wakabayashi, Yasuhiro Honda, Shoichi Iwamoto, “Dynamic Characteristics of Viscous-Friction Dampers by Simultaneous Vibration Displacement Measurement at Two Points, *SAE 2001 World Congress*, SAE Paper No. 2001–01–0281 (2001) P. 1–12.

[25] Tomoaki Kodama, Katsuhiko Wakabayashi, Yasuhiro Honda, Hiroshi Okamura, Shoichi Iwamoto, “An Investigation into Dynamic Characteristics of Torsional Viscous-Friction Dampers by Simultaneous Measurement at Two Points”, *Transactions of the Kokushikan University, Faculty of Engineering*, (in Japanese), No. 34 (2001) P. 23–31.

[26] Tomoaki Kodama, Katsuhiko Wakabayashi, Yasuhiro Honda, “an Experimental Study on the Dynamic Characteristics of Torsional Viscous-Friction Dampers for High-Speed Diesel Engine: Relationship between Damper Clearance and Kinematic Viscosity of Silicone Fluid” *Proceedings of the Japan Society of Mechanical Engineers, Dynamics and Design Conference 2001*, (in Japanese), No. 635 (2001) CD-ROM.

[27] Tomoaki Kodama, Katsuhiko Wakabayashi, Yasuhiro Honda, Shoichi Iwamoto, “An Experimental Study on the Dynamic Characteristics of Torsional Viscous-Friction Dampers: Behaviors of Damper Casing and Inertia Ring and Dynamic Characteristics of Damper”, *Proceedings of the Japan Society of Mechanical Engineers, 2001 Annual Meeting*, (in Japanese), No. F–0941 (2001) P. 107–180.

[28] B.I.C.E.R.A., “*A Handbook on Torsional Vibration*”, Cambridge at the University Press (1958), P. 520–558.

APPENDIX I

Relationship Between Rotary Coordinate System and Stationary Coordinate System (Refer to Fig. A–1)

Equation of motion of engine crankshaft system
 $[m] \cdot \ddot{L}(t) + [c] \cdot \dot{L}(t) + [k] \cdot L(t) = F(t)$ (A–1)

Equation of motion of rotary coordinate system
 $[m]_r \cdot \ddot{L}_r + [c]_r \cdot \dot{L}_r + [k]_r \cdot L_r - F_r - \omega \cdot [c] \times \alpha + [\omega^2 \cdot [m] \cdot [I_0] - \omega \cdot [c] \cdot [E]] \cdot r_{0,r}$ (A–2)

Where,

$$[E] = \begin{bmatrix} [E]_e & \cdots & 0 \\ \vdots & \ddots & \vdots \\ 0 & \cdots & [E]_e \end{bmatrix}$$

$$[I_0] = \begin{bmatrix} [I_0]_e & \cdots & 0 \\ \vdots & \ddots & \vdots \\ 0 & \cdots & [I_0]_e \end{bmatrix}$$

$$[E]_e = \begin{bmatrix} 0 & 0 & 0 & 0 & 0 \\ 0 & 0 & -1 & 0 & 0 \\ 0 & 1 & 0 & 0 & 0 \\ 0 & 0 & 0 & 0 & 0 \\ 0 & 0 & 0 & 0 & -1 \\ 0 & 0 & 0 & 0 & 1 \end{bmatrix}$$

$$[I_0]_e = \text{diag} [0, 1, 1, 0, 1, 1]$$

$$[m]_r = [m]$$

$$[c]_r = [c] + 2 \cdot \omega \cdot [m] \cdot [E]$$

$$[k]_r = [k] + \omega \cdot [c] \cdot [E] - \omega^2 \cdot [m] \cdot [I_0]$$

Where, $[m]$: mass matrix, $[c]$: damping matrix, $[k]$: stiffness matrix, $L(t)$: displacement vector, $F(t)$: forced vector
Harmonic forced vibration of i -th order vibration

$$F(t) = F_i \cdot e^{j\omega t} \quad (\text{A-3})$$

Displacement vector of i -th order vibration

$$L(t) = L_i \cdot e^{j\omega t} \quad (\text{A-4})$$

Equation of motion

$$([k] + j\omega \cdot [c] - (i\omega)^2) \cdot [m] \cdot L_i = F_i$$

$$[k_{dynamic} \cdot (i\omega)] = [k] + j\omega \cdot [c] - (i\omega)^2 \cdot [m] \quad (\text{A-5})$$

Where, ω : angular velocity, $[k_{dynamic} \cdot (i\omega)]$: stiffness matrix of i -th order vibration of crankshaft system

Vibration displacement of rotary coordinate system

$$[k_{dynamic} \cdot (i\omega)] \cdot L_i = F_i \quad (\text{A-6})$$

Stationary coordinate system: $Y-Z$, Rotary coordinate system: $y-z$

i -th order vibration of y, z direction of rotary coordinate system: l_y, l_z

Complex number of harmonic vibration

$$l_y = l_{y, Ri} \cdot \cos(i\omega t) + l_{y, i} \cdot \sin(i\omega t)$$

$$l_z = l_{z, Ri} \cdot \cos(i\omega t) + l_{z, i} \cdot \sin(i\omega t) \quad (\text{A-7})$$

i -th order vibration of Y, Z direction of stationary coordinate system: L_Y, L_Z

$(i+1), (i-2)$ th Order vibrations

$$L_Y = -[(l_{y, Ri+1} - l_{z, Ri+1} + l_{y, Ri-1} + l_{z, Ri-1}) \cdot \cos(i\omega) + (l_{y, Ri+1} + l_{z, Ri+1} + l_{y, Ri-1} - l_{z, Ri-1}) \cdot \sin(i\omega)]$$

$$L_Z = -[(l_{y, Ri+1} + l_{z, Ri+1} - l_{y, Ri-1} + l_{z, Ri-1}) \cdot \cos(i\omega) + (-l_{y, Ri+1} + l_{z, Ri+1} + l_{y, Ri-1} + l_{z, Ri-1}) \cdot \sin(i\omega)] \quad (\text{A-8})$$

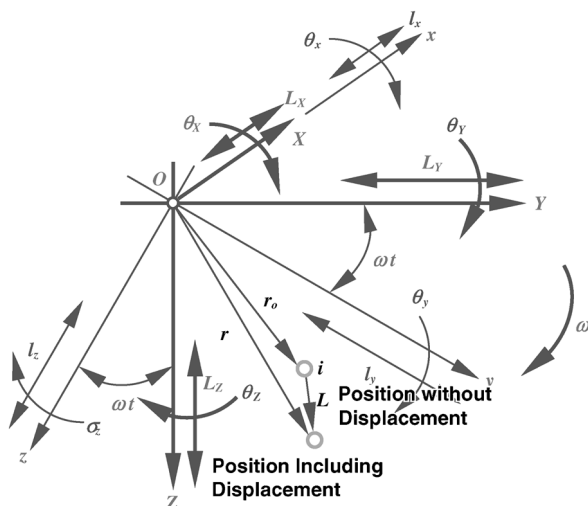


Fig. A-1 Rotary and Stationary Coordinate System

APPENDIX II

Bearing of Engine Crankshaft System (Refer to Fig. A-2)

Engine element, damping element of i -th order vibration of engine crankshaft system

Complex spring constant

$$k^* = k + j\omega c \quad (\text{A-9})$$

Where, k : equivalent elasticity coefficient of oil film, c : equivalent damping coefficient of oil film

Complex forced

$$F^* = k^* \cdot x^* \quad (\text{A-10})$$

Where, x^* : complex vibration displacement

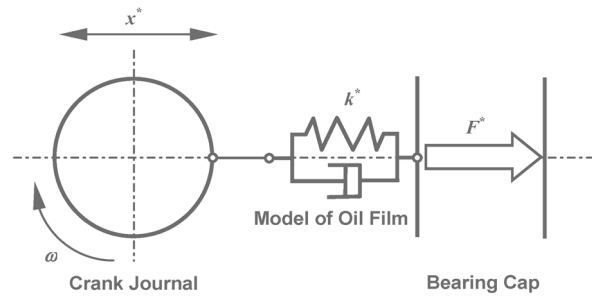


Fig. A-2 Idealized Model of Bearing